Supplementary Material for "A Comparative Study of the Domain Wall Motion in Ferrimagnets $(Fe,Co)_{1-x}(Gd,Tb)_x$"

Yuqing Zhou,[1] Teng Xu,[2, 3] Xue Liang,[1] Le Zhao,[2, 3] Heng-An Zhou[2,3], Zidong Wang[1], Wanjun Jiang,[2, 3, a)] and Yan Zhou[1, b)]

[1]*School of Science and Engineering, The Chinese University of Hong Kong, Shenzhen, Guangdong, 518172, China*

[2]*State Key Laboratory of Low-Dimensional Quantum Physics Department of Physics Beijing 100084, China*

[3]*Frontier Science Center for Quantum Information Tsinghua University Beijing 100084, China*

†Corresponding Authors.

[a)] E-mail: jiang_lab@tsinghua.edu.cn

[b)] E-mail: zhouyan@cuhk.edu.cn

Magnetic Properties Measurement Results

The anomalous Hall resistance of ferrimagnetic $(Co,Fe)_{1-x}(Gd,Tb)_x$ films with different compositions are measured at room temperature (300K). As shown in Fig. S1, all these ferrimagnetic films show strong perpendicular magnetic anisotropy. Here, the change of R_{AH} sign corresponds to the transition from being TM dominated to being RE dominated.

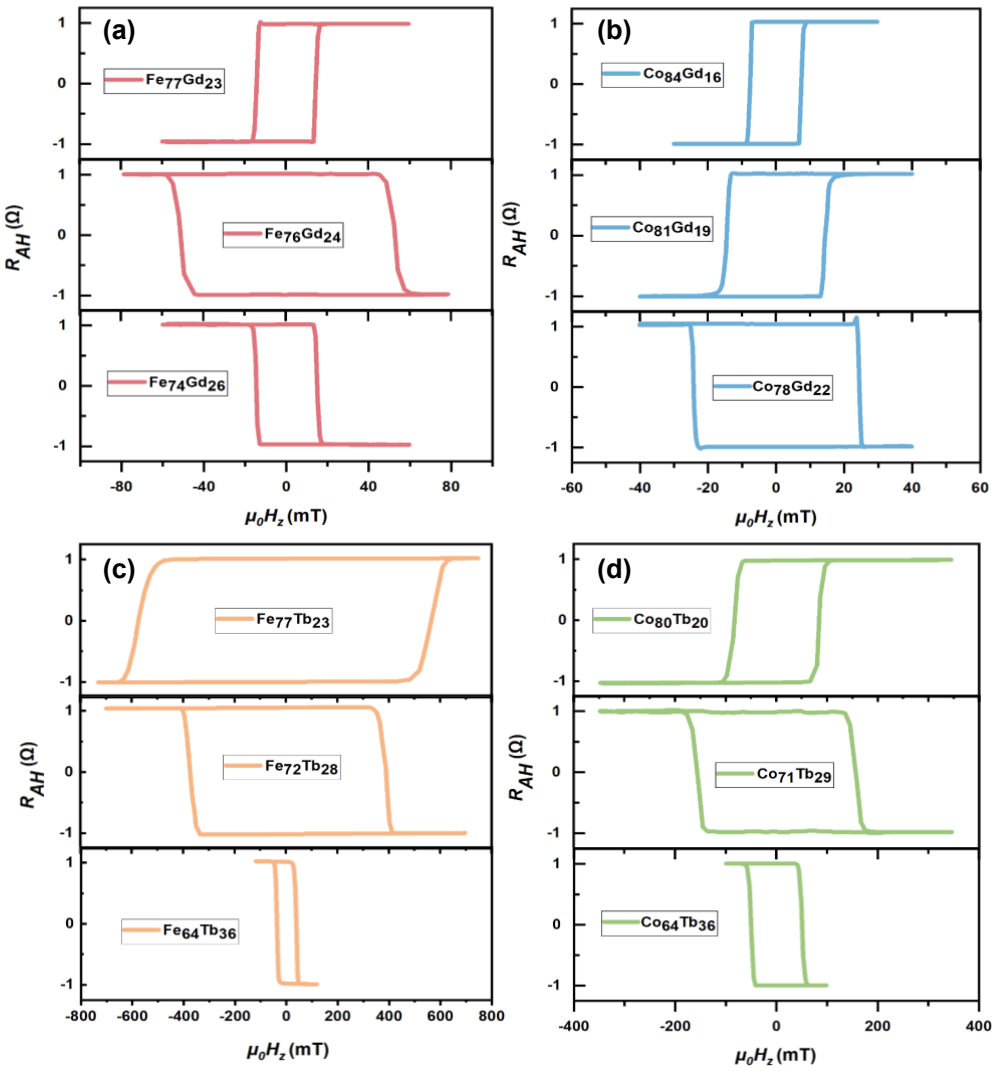

Fig. S1. Anomalous Hall resistance of ferrimagnets $(Fe,Co)_{1-x}(Gd,Tb)_x$ alloys with varying chemical compositions. All these measurements are performed at room temperature.

The perpendicular magnetic hysteresis loop of the selected ferrimagnetic samples is also measured.

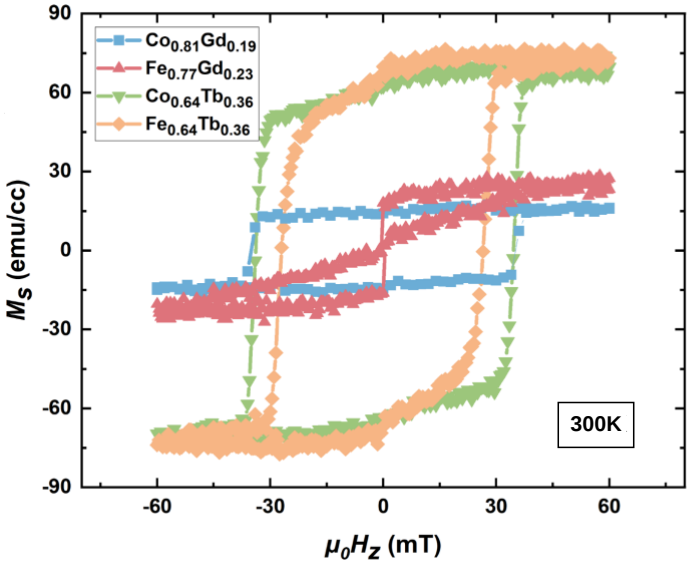

Fig. S2. Saturation magnetization measured by using vibrating sample magnetometry at room temperature (300K).

Micromagnetic Simulation Details

Micromagnetic simulations are performed by numerically solving the following coupled equations of motion in the presence of the spin-orbit torque:

$$\rho\dot{\boldsymbol{n}} = \boldsymbol{f}_m \times \boldsymbol{n} + \alpha(\rho\boldsymbol{n} \times \dot{\boldsymbol{m}} + \sigma\boldsymbol{n} \times \dot{\boldsymbol{n}}) + u_2\boldsymbol{n} \times (\boldsymbol{p} \times \boldsymbol{n}), \quad \text{(S1)}$$

$$\rho\dot{\boldsymbol{m}} + \sigma\dot{\boldsymbol{n}} = \boldsymbol{f}_m \times \boldsymbol{m} + \boldsymbol{f}_n \times \boldsymbol{n} + \alpha\rho\boldsymbol{n} \times \dot{\boldsymbol{n}} + u_1\boldsymbol{n} \times (\boldsymbol{p} \times \boldsymbol{n}), \quad \text{(S2)}$$

where $\boldsymbol{m} = (\boldsymbol{m_1} + \boldsymbol{m_2})/2$ and $\boldsymbol{n} = (\boldsymbol{m_1} - \boldsymbol{m_2})/2$ with $\boldsymbol{m_i}$ is the local unit magnetization for the sublattice *i*, respectively, $\rho = M_1/\gamma_1 + M_2/\gamma_2$, $\sigma = M_1/\gamma_1 - M_2/\gamma_2$, $u_1 = \beta_1 + \beta_2$, $u_2 = \beta_1 - \beta_2$ with $\beta_i = \mu_B\theta_{\mathrm{SH}}j/\gamma_i e t_z$, α is the Gilbert damping constant and $\boldsymbol{p}$ is the spin polarization direction. M_i and γ_i are the saturation magnetization and the gyromagnetic ratio for the sublattice *i*, respectively, j is the current density, μ_B is the Bohr magneton, θ_{SH} is the spin Hall angle of the spin current, e is the electron charge and t_z is the thickness of the film. $\boldsymbol{f}_m = -\frac{\delta\varepsilon}{\mu_0\delta\boldsymbol{m}}$ and $\boldsymbol{f}_n = -\frac{\delta\varepsilon}{\mu_0\delta\boldsymbol{n}}$ are the effective fields

induced by various interactions within the system, such as the exchange interaction, DMI and the perpendicular magnetic anisotropy. Here, the total energy density in the continuum approximation can be written as

$$\varepsilon = \frac{\lambda}{2}\boldsymbol{m}^2 + \frac{A}{2}(\partial_x \boldsymbol{n})^2 - \frac{K}{2}(\boldsymbol{n}\cdot\boldsymbol{e}_z)^2 + \frac{D}{2}\boldsymbol{e}_y\cdot(\boldsymbol{n}\times\partial_x\boldsymbol{n}) - \mu_0 M_s \boldsymbol{H}\cdot\boldsymbol{n}, \qquad \text{(S3)}$$

where λ and A are the homogeneous and inhomogeneous exchange constants, respectively. K is the perpendicular magnetic anisotropy constant. D denotes the interfacial DMI. M_S is the total magnetization and $\boldsymbol{H}$ is the external magnetic field.

Theoretical Approach Details

Substituting $\boldsymbol{f}_m = -\frac{\lambda}{\mu_0}\boldsymbol{m}$ into Eq. (S1) and (S2), one can obtain the closed equation in terms of the Néel vector **n**, and $\boldsymbol{f}_{\boldsymbol{n}}$

$$\frac{\mu_0\rho^2(1+\alpha^2)}{\lambda}\boldsymbol{n}\times(\boldsymbol{n}\times\ddot{\boldsymbol{n}}) = \sigma\boldsymbol{n}\times\dot{\boldsymbol{n}} + \alpha\rho\dot{\boldsymbol{n}} + u_1\boldsymbol{p}\times\boldsymbol{n} - \boldsymbol{n}\times(\boldsymbol{f}_{\boldsymbol{n}}\times\boldsymbol{n}) - \frac{\mu_0 u_2\rho}{\lambda}\boldsymbol{n}\times(\boldsymbol{p}\times\dot{\boldsymbol{n}}). \qquad \text{(S4)}$$

We use the collective coordinate approach proposed by A.A. Thiele [S1] to derive the steady velocity of a domain wall. Here, Walker ansatz [S2] is used to describe the domain wall profile, i.e., $\boldsymbol{n}(x,t) = (\sin\theta\cos\phi, \sin\theta\sin\phi, \cos\theta)$, where $\theta = 2\arctan\{\exp[(x-r)/\Delta]\}$ and Δ is the DW width. Taking the scalar product of Eq. (S4) with $\partial_r\boldsymbol{n}$ and integrating over the whole film, we can obtain the following motion equations

$$\frac{\mu_0\rho^2(1+\alpha^2)}{\lambda}\mathcal{M}\ddot{r} = -2\sigma\dot{\phi} - \alpha\rho\mathcal{M}\dot{r} + \frac{2M_S H_z}{\mu_0} + \pi u_1\cos\phi, \qquad \text{(S5)}$$

Here, $\boldsymbol{p}$ is set to be $\boldsymbol{e}_y$ and $\mathcal{M} = \int(\partial_r\boldsymbol{n}\cdot\partial_r\boldsymbol{n})dx \approx \frac{2}{\Delta}$ is determined by the magnetic structure in a DW. For a steady motion under the Walker breakdown, DW does not precess so that $\dot{\phi}$ remains 0, and $\ddot{r}$ should also be zero. Therefore, the steady velocity of the Néel wall [S3,S4] is given as

$$v = \dot{r} = \frac{1}{\alpha\rho\mathcal{M}}\left(\frac{2M_S}{\mu_0}H_z + \pi u_1\cos\phi\right) \approx \frac{\Delta}{2\alpha\rho}\left(\frac{2M_S}{\mu_0}H_z + \pi u_1\cos\phi\right). \qquad \text{(S6)}$$

Micromagnetic Simulation Results of the DW Motion Driven by the Current Pulse with a Perpendicular Field (H_z)

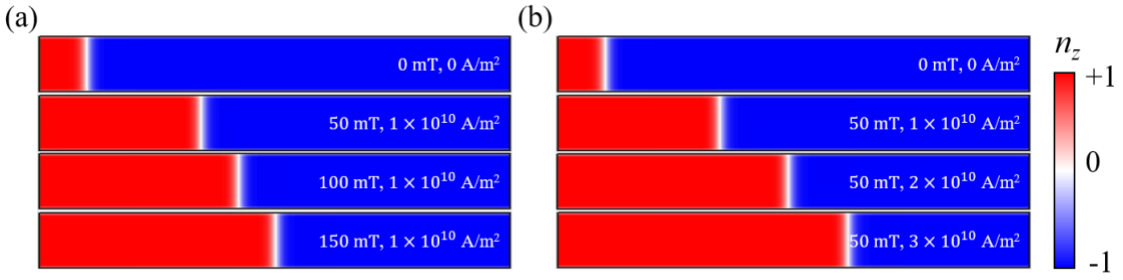

Fig. S3. Micromagnetic simulation snapshots of the domain configurations driven by (a) the different perpendicular fields (H_z) with a current pulse at a fixed density. (b) the fixed perpendicular fields with a current pulse at different densities. The DW motion is along the x-direction. Here, a 1000-nm-long ferrimagnetic nanotrack is considered with the parameters: λ = 96 MJ/m^3, A = 6 pJ/m, D = -0.35 mJ/m^2, K = 26 kJ/m^3, M_1 = 150 kA/m, M_2 = 135 kA/m, $M_s = M_1 - M_2$ = 15 kA/m, γ_1 = 2.211 × 10^5 m/(A·s), γ_2 = 1.1 γ_1, α = 0.05.

Micromagnetic Simulation Results of the DW Motion Driven by the Current Pulse with an In-plane Field (H_x)

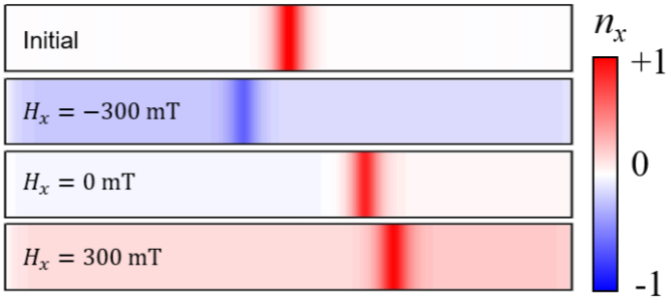

Fig. S4. Micromagnetic simulation snapshots of the domain configurations driven by different in-plane fields (H_x) with current pulses at a fixed density. λ = 96 MJ/m^3, A = 6 pJ/m, D = -0.1 mJ/m^2, K = 26 kJ/m^3, M_1 = 150 kA/m, M_2 = 135 kA/m, $M_s = M_1 - M_2$ = 15 kA/m, γ_1 = 2.211 × 10^5 m/(A·s), γ_2 = 1.1 γ_1, α = 0.05.

References

[S1] A. Thiele, Phys. Rev. Lett. 30, 230 (1973).

[S2] N. L. Schryer and L. R. Walker, J. Appl. Phys. 45, 5406–5421 (1974).

[S3] T. Shiino, S.-H. Oh, P. M. Haney, S.-W. Lee, G. Go, B.-G. Park, and K.-J. Lee, Phys. Rev. Lett. 117, 087203 (2016).

[S4] S.-H. Oh, S. K. Kim, D.-K. Lee, G. Go, K.-J. Kim, T. Ono, Y. Tserkovnyak, and K.-J. Lee, Phys. Rev. B 96, 100407(R) (2017).